Am J Physiol Gastrointest Liver Physiol 293: G532–G543, 2007.
First published June 14, 2007; doi:10.1152/ajpgi.00138.2007.

Modulatory role of phosphoinositide 3-kinase in gastric acid secretion

S. E. Mettler, S. Ghayouri, G. P. Christensen, and J. G. Forte
Department of Molecular and Cell Biology, University of California, Berkeley, California

Submitted 27 March 2007; accepted in final form 9 June 2007

Mettler SE, Ghayouri S, Christensen GP, Forte JG. Modulatory role of phosphoinositide 3-kinase in gastric acid secretion. *Am J Physiol Gastrointest Liver Physiol* 293: G532–G543, 2007. First published June 14, 2007; doi:10.1152/ajpgi.00138.2007.—The gastric parietal cell is responsible for the secretion of HCl into the lumen of the stomach mainly due to stimulation by histamine via the cAMP pathway. However, the participation of several other receptors and pathways have been discovered to influence both stimulation and inhibition of acid secretion (e.g., cholinergic). Here we examine the role of phosphoinositide 3-kinase (PI3K) in the modulation of acid secretion. Treatment of isolated gastric glands and parietal cells with the PI3K inhibitor, LY294002 (LY), potentiated acid secretion in response to histamine to nearly the maximal secretion obtained with histamine plus phosphodiesterase inhibitors. As cAMP levels were elevated in response to histamine plus LY, but other means of elevating cAMP (e.g., forskolin, dbcAMP) were not influenced by LY, we posited that the effect might require activation of G-protein-coupled histamine H_2 receptors, possibly through the protein kinase B pathway (also known as Akt). Study of downstream effectors of PI3K showed that histaminergic stimulation increased Akt phosphorylation, which in turn was blocked by inhibition of PI3K. Expression studies showed that high expression of active Akt decreased acid secretion, whereas dominant-negative Akt increased acid secretion. Taken together, these data suggest stimulation with histamine increases the activity of PI3K leading to increased activity of Akt and decreased levels of cAMP in the parietal cell.

parietal cell; Akt; protein kinase B; phosphodiesterase; H-K-ATPase

A PRIMARY PATHWAY FOR ACTIVATION of the gastric oxyntic cell is via histamine H_2-receptor stimulation, activation of a G-protein coupled receptor (GPCR), adenylyl cyclase activation, cAMP production, and recruitment of proton pumps (H-K-ATPase) into the apical plasma membrane through cAMP-dependent protein kinase (PKA) and other downstream protein kinases (8, 10–12, 14, 18). However, additional pathways for direct activation (e.g., cholinergic) and for negative and positive modulation of the histamine/cAMP pathway are clearly extant and appear to cooperate to relatively variable degrees depending on the vertebrate species and on the particular oxyntic cell preparation used to study (4, 13, 26, 31). The overall conclusion from these published data is that the signaling system for acid secretion is a complex set of interactions with cellular vegetative functions, including energy metabolism, membrane synthesis and degradation, cell growth, cell migration, and cellular connectivity.

In this study we have used the rabbit gastric parietal cell as the oxyntic cell model to evaluate the modulating role of an important cellular signaling regulator, phosphoinositide 3-kinase (PI3K), on the histamine-stimulated path for activation of acid secretion. PI3K is a lipid kinase responsible for phosphorylating the D-3 position of phosphatidylinositol (36). PI3K mainly produces phosphoinositide 3,4,5-phosphate (PIP_3) from phosphoinositide 4,5-phosphate (PIP_2). Activation of the class IB PI3K is generally attributed to the Gβγ-subunit of heterotrimeric G proteins (37). PI3K has been shown to be involved in cell signaling and growth, DNA synthesis, survival, migration, and endocytosis. In addition, there is now strong evidence that activation of PI3K in adipocytes, pancreatic β cells, and cardiomyocytes leads to the phosphorylation of protein kinase B (also known as Akt) and the subsequent activation of phosphodiesterase (PDE), resulting in a decreased cAMP level (16, 21, 41). The work here is directed toward understanding our initial observed potentiation of the acid secretory response to histamine when PI3K was inhibited. The data suggest that parietal cell PI3K is activated by the Gβγ-subunits of histamine-stimulated G-protein coupled receptor. Active PI3K activates downstream Akt, ultimately enhancing the activity of cAMP-PDE, which limits the cellular level of cAMP, especially at limiting rates of cAMP production. We propose that this PI3K pathway may be a physiological modulator of cellular energy commitment to acid secretion at low levels of stimulation.

MATERIALS AND METHODS

Materials. Ketamine and xylazine were from Vetus Animal Health, Westbury, NY. Nembutal was from Premier Pharmacy Labs. Dulbecco's phosphate-buffered saline, Minimal essential medium, and DMEM F-12 were from Gibco/Invitrogen, Grand Island, NY. Collagenase was from Worthington Biochemical, Lakewood, NJ. Aminopyrine (AP) was from GE Healthcare Life Sciences. Epidermal growth factor (EGF) was from BD Biosciences, Bedford, MA. Glutamine, dibutyryl-cAMP, carbachol, SITE liquid medium, histamine, and novobiacin were from Sigma, St. Louis, MO. Gentamycin was from Cellgro, Herndon, VA. MatriGel was from Collaborative Biomedical, Bedford, MA. Forskolin was from Alexis Biochemicals, Lausanne, Switzerland. Lupitidine was from Smith Kline and French Laboratories, Welwyn Garden City, Herts, UK. Cimetidine was from Abbott Laboratories, Chicago, IL. LY294002 (LY), anti-Akt isoforms 1 and 2, and anti-Akt phosphor serine-473 were from EMD/Calbiochem, San Diego, CA. Anti-H-K-ATPase (2G11) was obtained from Affinity Bioreagents, Golden, CO. All reagents were dissolved in water except for LY, wortmannin, and forskolin. These latter three were dissolved in DMSO for addition to the biological preparations. Electrophoresis-grade chemicals were from Bio-Rad. All electron microscopy grade materials were from Electron Microscopy Sciences, Fort Washington, PA. HitHunter cAMP Kit was from DiscoveRx, Fremont, CA. All other reagents were from standard suppliers and were of the highest purity.

Tissue collection. Tissue collection was performed as described by Zhou et al. (42). All protocols and procedures were reviewed and approved by the Berkeley Animal Care and Use Committee. Briefly,

Address for reprint requests and other correspondence: J. G. Forte, Dept. of Molecular and Cell Biology, Univ. of California, Berkeley, CA 94720-3200 (e-mail: jforte@berkeley.edu).

The costs of publication of this article were defrayed in part by the payment of page charges. The article must therefore be hereby marked "*advertisement*" in accordance with 18 U.S.C. Section 1734 solely to indicate this fact.

New Zealand White rabbits were used as the source of gastric glands and isolated parietal cells. Rabbits were injected subcutaneously with 20 mg/kg of cimetidine 1 h before the procedure. High-pressure perfusion of the stomach was performed for 5–10 min using oxygenated, 37°C, Dulbecco's phosphate-buffered saline. The gastric mucosa was separated from the underlying muscle layer and washed, followed by digestion for 30 min at 37°C with 25 mg collagenase type 4 (257 U/mg) in 30 ml HEPES-MEM containing 20 mg bovine serum albumin (BSA). A 1:10 dilution of the collagenase with HEPES-MEM stopped the digestion. Glands were allowed to settle for 15 min, and cells remained in suspension. The settled glands were washed and resettled three times with HEPES-MEM. A final suspension of glands was made to 2.5% cytocrit in HEPES-MEM. The suspended cells were used for studies on cultured parietal cells (described later).

AP assay on gastric glands. AP assays were used as an indirect method of evaluating acid secretion. AP assays are based on accumulation of AP in acidic spaces and were carried out as described by Berglindh et al. (5, 6). Briefly, 1 ml of a 2.5% gland suspension in HEPES-MEM was placed in preweighed tubes containing various stimulants and inhibitors along with 10 μl of [^{14}C]AP (115 mCi/mmol) containing about 5×10^3 cpm. The tubes were buzzed with 100% oxygen, capped, and incubated in a 37°C shaking water bath for 20–30 min. The glands were pelleted, and 200 μl of supernatant put into 3 ml of scintillation fluid and counted with a Beckman LS3801 counter. The remaining supernatant was removed, and the pelleted glands dried overnight at 80°C. The tubes were weighed to calculate the dry weight, and 100 μl of 1 M NaOH was added to the pellet. After incubation with NaOH for 20 min at 80°C, 100 μl of 1 M HCl was added to neutralize the suspended pellet. All 200 μl were placed in scintillation fluid and counted. The AP ratio was calculated using the equation [(Pellet cpm)/((Pellet g) × C)]/(Supernatant cpm/1 μl), where pellet weight is dry weight in grams. Berglindh and Öbrink (6) determined the conversion factor, C, used to estimate volume from dry weight as 2,000 μl/1 g. For reporting data here, the AP ratio was normalized so that resting glands (500 μl lupitidine treatment) for any given experiment was set to 1.0.

Plating cells and glands. Isolated gastric glands for culture were diluted to 1% in medium A [DMEM/F-12 medium, 4.77 g/l HEPES, 0.2% BSA, 10 mM glucose, 50 ng/ml EGF, 5% selenite-insulin-transferrin (SITE) liquid medium, 1 mM glutamine supplement, 50 U/ml penicillin/streptomycin, 200 μg/ml gentamycin, and 50 μg/ml novobiacin], pH 7.4, and plated onto Matrigel-coated coverslips and incubated at 37°C.

Isolated gastric cells taken as the supernatant from the mucosal digestion described above were pelleted by centrifugation at 200 *g*, washed three times with HEPES-MEM, and finally resuspended in medium A. Approximately 70% of the total gastric cells suspended in medium A were parietal cells. The cells were plated onto either Matrigel-coated 18-mm round coverslips or onto 35-mm dishes and incubated at 37°C.

AP assay on cultured glands. Glands were cultured on 22-mm square coverslips for 42 h, rinsed with 37°C MEM, and placed in 1 ml of fresh medium A. Cultures were treated with various drugs, including 10 μl of [^{14}C]AP, and incubated for 30 min at 37°C. Coverslips were removed from the media, quickly dipped in warm MEM, blotted, and placed in 2× SDS sample buffer for 1 h. [^{14}C]AP counts were measured for both the incubation supernatant and the SDS-solubilized cell scrapings. Protein concentration for each sample was determined using the filter paper assay.

Filter paper assay. Known dilutions of ovalbumin were made in sample buffer, and 4-μl spots were placed on a number 1 filter paper along with solubilized unknown samples (4 μl) and allowed to dry for 20 min. The filter paper was washed with methanol for 1 min. The filter paper was allowed to dry and stained with 0.5% Coomassie blue G250 in 7% acetic acid for 20 min. Excess stain was removed with several changes of Destain II (19% ethanol and 7% acetic acid). The paper was allowed to dry and scanned into a computer file. The area and density of each spot was determined and compared with the ovalbumin standards to obtain the protein concentration of each sample.

Differential-interference contrast imaging. Cells were plated on Matrigel-coated, glass-bottom microwell dishes (Mat Tek) and allowed to settle overnight at 37°C. The medium A was changed after 18 h, and the cells cultured for another 24 h. The cells were maintained at 37°C with a stage warmer (Warner Instruments) while being viewed with a Nikon Eclipse TE2000-U inverted microscope equipped with an automatic XY stage positioner. Differential-interference contrast (DIC) images were acquired for eight areas per well immediately prior to the addition of drugs (to represent resting cells) and every 5 min after treatment with stimulants over the course of 25 min. NIH Image 1.63 software was used to determine the change in vacuole area over the 25 min of treatment.

Adenoviral infections. Recombinant adenoviruses with incorporated constructs of hemagglutinin (HA) tagged Akt were used to get the cells to express various forms of Akt protein in parietal cells. The constructs were a kind gift from Dr. K. Walsh (19) and included wild-type mouse Akt (WT-Akt), myristoylated Akt (Myr-Akt), and Akt mutated by substitutions at Lys179Ala, Thr308Ala, and Ser473Ala (AAA-Akt), all under the control of the CMV promoter. Viruses were amplified according to Fujio et al. (19) except that Bosc 23 cells (a kind gift from Dr. T. Machen, Berkeley) cultured in DMEM with 4.5 g/l glucose, sodium pyruvate, and L-glutamine, 10% fetal calf serum, 1% penicillin and streptomycin, with 5% CO_2 balanced air at 37°C, were used as opposed to HEK 293 cells, and virus was purified by ultracentrifugation of cell lysates. Infection of gland cultures was tested using two different concentrations of viral supernatant followed by examination of glandular cells by immunostaining with an anti-HA antibody. The lower of the two doses was found to produce protein expression in greater than 90% of the cells and was used for further experiments. Experimental infections were performed 3–5 h after the initial plating and cultured ~18 h; at that point the medium A was replaced and cultured for an additional 24 h.

Western blot analyses. Glands or cells solubilized in SDS sample buffer were loaded onto 12.5% acrylamide gels for SDS-PAGE. After developing the gel, the proteins were transferred to nitrocellulose membranes using a wet transfer apparatus and subsequently blocked in either 10% milk in PBST (PBS and 0.05% Tween 20) or 5% BSA in TBST (10 mM Tris base, 150 mM NaCl, and 0.05% Tween 20). Blots were probed with mouse antibody against Akt phosphorylated at Ser^{473} (Calbiochem, diluted 1:200) in TBST with 2% BSA, followed by secondary probing with HRP-tagged goat anti-mouse IgG (Jackson, diluted 1:5,000) in TBST with 2% BSA. Bands were developed using the Western Lightning Chemiluminescence Reagent Plus (PerkinElmer LAS), and film was scanned and analyzed using NIH Image to determine relative levels of phosphorylated Akt. Blots were stripped in stripping buffer (62.5 mM Tris·HCl, 2% SDS, and 100 mM 2-mercaptoethanol) for 30 min at 50°C and used for reprobing with rabbit anti-Akt isoforms 1 and 2 (Santa Cruz Biotechnology, 1:200) to determine total Akt, or mouse anti-H-K-ATPase β-subunit 2G11 (1:4 in PBS with 2% BSA), followed by HRP-tagged goat anti-rabbit or HRP-tagged goat anti-mouse IgG (Jackson, diluted 1:5,000 in PBS with 2% BSA).

cAMP assay. Freshly isolated glands were treated with various stimulants and inhibitors. Glands were allowed to settle, and the supernatant was removed, and the glands were frozen in liquid nitrogen within 2 min of removal from the incubator. Glands were subjected to shearing in 500 μl of ice-cold 6% TCA. The protein was pelleted via centrifugation, dried, and weighed. The TCA in the supernatant was extracted with ether and then dried down in a speed vac and resuspended in 40 μl of 50 mM sodium acetate, pH 4.7. The remaining part of the immunoassay was performed as per HitHunter cAMP Kit instructions. Briefly, the cAMP extracted from the glands was mixed with cAMP antibody and incubated at room temperature for 1 h. The fluorescent substrate and the enzyme donor were mixed

together and incubated for 1 h at room temperature. The enzyme acceptor was added and incubated for 1–3 h at room temperature. The reaction was stopped with the addition of the stopping solution, and the relative fluorescent units were determined using a fluorimeter. Samples were excited at 530 nm, and an emission spectrum was collected from 540 nm to 640 nm. The peak emission was between 586 and 587 for all samples. The relative fluorescence units for each sample were compared with the linear range of a standard cAMP curve to determine the approximate cAMP concentration in the experimental samples.

Chemical fixation for TEM. Freshly isolated gastric glands stimulated in the same fashion as for the AP assays were allowed to settle and then washed with 0.1 M sodium cacodylate, pH 7.2. The glands were fixed with 2% glutaraldehyde in 0.1 M sodium cacodylate, pH 7.2, for 24 h at 4°C and washed three times with 0.1 M sodium cacodylate. Glands were postfixed with 1% osmium tetroxide in 0.1 M sodium cacodylate for 1 h at room temperature followed by three 5 min sodium cacodylate washes and three 10 min distilled water washes. En bloc staining was performed with 0.5% uranyl acetate overnight at 4°C. Uranyl acetate was washed out with three washes with distilled water followed by serial dehydration in graded acetone. The samples were infiltrated with constant rotation using 2 to 1, 1 to 1, and 1 to 2 mixtures of acetone to eponate resin followed by 1 h of pure resin, then overnight with fresh resin, all at room temperature. Then fresh resin with accelerator was added and allowed to cure for 2 days at 60°C.

TEM imaging. Blocks were sectioned on a RMC MTX ultramicrotome. Approximately 20 sections were cut of the appropriate TEM thickness of 60–70 nm yielding a silver to gold color. The thin sections were collected on Formvar and carbon-coated 100 mesh copper grids. Thin sections were stained with 2% uranyl acetate in 70% methanol for 10 min and washed with 5 rinses each of 70%, 50%, and 30% methanol followed by 9 rinses of distilled water. Next the grids were stained with Reynolds lead citrate for 5 min and rinsed 9 times with distilled water. The Philips Technai 12 TEM was used to view the thin sections at 100 kV.

Quantitative stereology. Images of well-preserved parietal cells, as determined by examining the general morphology, containing a portion of the nucleus, apical membrane, and basolateral membranes were taken at a magnification of 9,300× on a Technai 12 TEM at 100 kV and were subjected to quantitative stereology (7, 20). Surface area was calculated using a test screen with staggered test lines of 4 cm in length, separated by 3 cm horizontally and 3 cm longitudinally. Surface area (S) of microvilli, tubulovesicles, and apical and basolateral membranes were derived from the number of intersections (I) between the testlines and the membranes. For surface area determination (S) the variables were related by the equation, $S = 2 \times (I/L)$, where L is half the number of endpoints multiplied by the length and I is as stated above. Volume densities (V) were determined by placing a lattice of grid-test points (0.65 cm grid) placed onto micrographs and determining the fraction of points (P) enclosed within the specified structure, to the total number of points P_{total}, related by the equation, $V = P/P_{total}$.

RESULTS

Inhibition of PI3K increases histamine-stimulated acid secretion. An increase of histamine-stimulated AP accumulation (our index of acid secretion) was observed when a well-known inhibitor of PI3K, LY, was included in the gland incubation medium. A similar increase of histamine-stimulated AP accumulation was observed previously with the use of the PI3K inhibitor wortmannin (25). Control experiments with the DMSO vehicle showed no changes in AP accumulation. The AP uptake data of Fig. 1 compare the glandular secretory response to histamine alone and when LY and the PDE inhibitor IBMX were included along with histamine for a large number of experiments. For each experiment shown in Fig. 1, the AP data were normalized by setting the value of nonstimulated, lupitidine-treated glands to 1.0 and by measuring the relative increase with subsequent treatments. Lupitidine is a histamine H_2 receptor-blocker that is reportedly ten times more active than cimetidine at inhibiting acid secretion stimulated by histamine in vivo (9). Lupitidine dose response assays were performed on gland preparations treated with 200 μM histamine, and an IC_{50} of 104 μM was determined (data not shown). Control experiments with somewhat smaller *n* value were also included for the effects of LY alone and LY added in the presence of lupitidine. Glands stimulated with 200 μM histamine (H) alone had a mean AP accumulation index of 4.2 ± 0.3-fold over resting glands maintained in the resting state with Lup. When IBMX was included with histamine (H+I), AP accumulation was elevated to 9.4 ± 0.8-fold over resting levels. These conditions of H+I are essentially the maximum acid secretory response of the isolated gastric glands (32). When the PI3K inhibitor LY was included with histamine (H+LY), gastric glands were stimulated 8.9 ± 0.8-fold over resting glands, more than two times the response to H alone and close to the same level as H+I ($P < 0.01$). LY did not increase AP accumulation of resting glands, nor did it significantly alter the maximal stimulation observed with histamine plus IBMX. A detailed time course of AP accumulation showed that the stimulatory response to histamine alone reached a plateau after only 5 min of treatment, whereas glands treated with histamine + IBMX or with histamine + LY continued to increase AP accumulation with nearly identical kinetics over the 30 min period of study (data not shown).

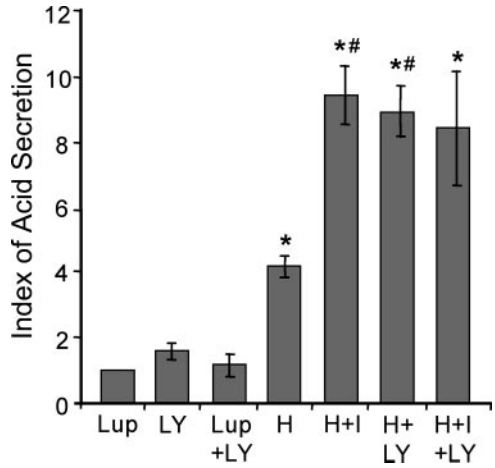

Fig. 1. LY294002 increases histamine-stimulated acid secretion by gastric glands over that produced by histamine alone. The aminopyrine (AP) uptake assay was used as an index of acid secretion and normalized for each experiment relative to the AP uptake of freshly isolated glands held in the nonsecreting (resting) state with 500 μM lupitidine (Lup). Addition of 200 μM histamine (H) stimulated acid secretion, and that is greatly enhanced by including 60 μM IBMX plus 200 μM histamine (H+I). Addition of 20 μM LY294002 plus 200 μM histamine (H+LY) also stimulated acid secretion more than histamine alone. LY294002 did not increase acid secretion of resting (Lup+LY) or maximally stimulated glands (H+I+LY). Error bars represent the standard error of the mean SE. *$P < 0.01$ with respect to Lup, #$P < 0.01$ with respect to H alone; $n > 10$ for Lup, H, H+I, H+LY, H+I+LY; $n = 3$ for LY and Lup+LY.

Increased acid output is confirmed for two independent PI3K inhibitors. LY was reported to inhibit PI3K and not to inhibit PI-4-kinase, EGF receptor tyrosine kinase, or PKC when used at 50 μM (38). The dose response to LY and to that of another well-known PI3K inhibitor, wortmannin, are compared in Fig. 2. Although the potencies of the two drugs for AP uptake were markedly different, both PI3K inhibitors caused a biphasic response on top of the normal stimulatory response to histamine, with a stimulatory effect at low dose and inhibition at higher levels. For LY, the enhancement of histamine stimulation began at 5 μM with maximal stimulation at 40 μM; frank inhibition occurred above 100 μM. Wortmannin maximally enhanced histamine-stimulated AP uptake at the much lower dose of 0.1 μM and began to inhibit acid secretion above 2.5 μM. Wortmannin is known to block both the ATP and $PI(4,5)P_2$ binding sites of PI3K by covalently modifying lysine-802 of the p110 catalytic subunit, resulting in a highly potent inhibitor (IC_{50}, 2 nM) (40). LY, on the other hand, simply blocks the ATP binding site, resulting in a higher concentration required for inhibition of PI3K (IC_{50}, 1.4 μM; Ref. 38). However, the IC_{50} values for wortmannin and LY referenced here were obtained by in vitro methods and may not represent the exact values in vivo.

Morphology confirms enhanced histamine stimulation with PI3K inhibition. The AP uptake data clearly suggest that inhibition of PI3K results in increased histamine-stimulated acid secretion. To confirm that this was indeed a real parietal cell secretory response, alternative means to confirm the enhanced secretory state were used. Thus, morphological studies were performed at both the light and electron microscope levels by which we visualized definitive parietal cell responses to stimulation.

For the studies with the light microscope, parietal cells isolated from rabbit gastric mucosa were used. Rabbit parietal cells grown in culture take on a different morphology than in vivo (2, 42). After a few hours in culture the apical membrane including the secretory canaliculi becomes closed to the outside environment, ultimately forming vacuoles that we refer to as apical membrane vacuoles. The outside plasma membrane is referred to as the basolateral membrane and is the site of histamine-receptor-mediated stimulation. During stimulation H-K-ATPase-rich cytoplasmic tubulovesicles are transported to and fuse with the apical membrane vacuoles, and HCl and water are pumped into the vacuole where notable swelling can be observed (2, 24). A time course of the morphological changes in cultured parietal cells during 25 min of stimulation with H, H + IBMX, or H + LY was carried out. As exemplified in Fig. 3, *A–L*, stimulation caused a progressive enlargement of apical vacuoles. In some cases multiple small apical vacuoles would appear to fuse together and become a single larger vacuole; in other cases vacuoles simply appeared to swell. No change in vacuole size occurred with LY alone. To quantify and compare the relative changes, images were recorded at periodic intervals and used to measure the increase in vacuole area per cell as an index of swelling volume. The total vacuole area per cell, measured at 0 and 25 min, and the percent change for each stimulant are shown in Table 1. Histamine alone induced an increase in vacuole area by 136% ± 15%, significantly less than the increase of 219% ± 32% caused by H + LY ($P < 0.05$). The measured increase in vacuole area for H + IBMX was 171% ± 19%, not significantly different from the increase caused by histamine + LY (Table 1).

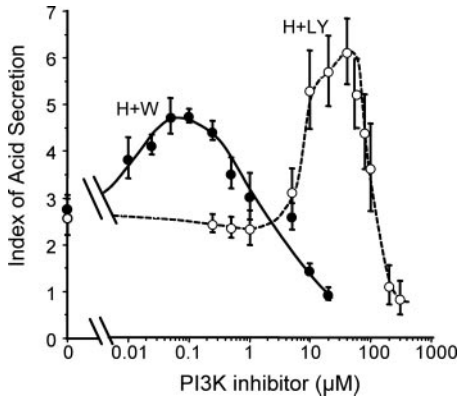

Fig. 2. Phosphoinositide 3-kinase (PI3K) inhibitors increase histamine-stimulated acid secretion. Glands were held in the resting state with 500 μM Lup, AP ratio set at 1.0. Additional glands were stimulated with 200 μM H plus increasing concentration of LY294002 (H+LY), or alternatively with H plus increasing concentration of wortmannin (H+W). Both PI3-kinase inhibitors, LY and wortmannin, have biphasic effects on histamine-stimulated acid secretion: enhancement at low concentrations and inhibition at high concentrations. Stimulation with H+I resulted in 8.61 ± 1.12-fold over resting levels. Error bars represent the SE; $n > 10$ for Lup and H+I, $n \geq 4$ for all LY concentrations, and $n = 3$ for all wortmannin concentrations.

Light microscopy provided information on large vacuolar expansion resulting from the addition of agonists, but transmission electron microscopy is necessary to observe fine ultrastructural detail of parietal cells, including the tubulovesicles and the apical canalicular membranes. Representative micrographs of parietal cells from glands in the resting condition and those treated with various agonists are shown in Fig. 4. Casual examination revealed few differences between resting glands (Fig. 4*A*) and histamine-stimulated glands (Fig. 4*B*), both of which contained numerous tubulovesicles in the cytoplasm and limited apical microvilli and canalicular space. However, for glands treated with H + IBMX (Fig. 4*C*) or H + LY (Fig. 4*D*) there were rather striking morphological transformations, e.g., a large decrease in tubulovesicles and an increase in apical microvilli and canalicular space.

The results of quantitative stereology for all glandular treatments are given in Table 2. For histamine-treated glands, parietal cells showed a small decrease in percent volume of tubulovesicular space and correspondingly small increases in microvillar and canalicular percent volumes compared with resting glands, but these changes did not reach the 5% level of significance. Parietal cells from glands stimulated with histamine + IBMX demonstrated large and significant changes in morphology and membrane transformation. Surface density of tubulovesicles decreased about 5-fold ($P < 0.05$), and there was an equivalent 5-fold increase in apical and microvillar membrane surface density ($P < 0.01$). Parietal cells in glands treated with histamine + LY also displayed large morphological transformations (though not as great as histamine + IBMX) with about 2.5-fold decrease in surface density ($P < 0.01$) and 3-fold increase in combined apical and microvillar membrane surface density ($P < 0.01$). For all treatments there was conservation of membrane within parietal cells such that the increase in total apical surface was accounted for by the loss of tubulovesicular membrane area. Also, the basolateral

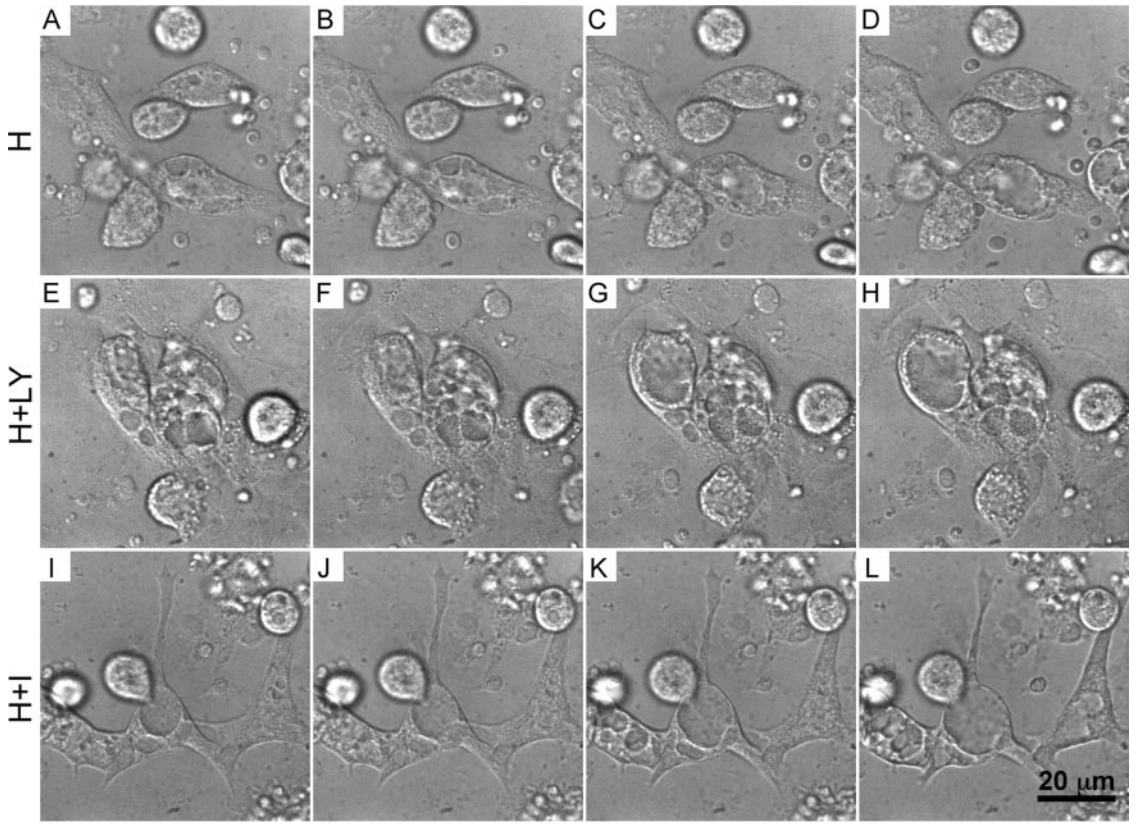

Fig. 3. H+LY induces a greater acid secretion and swelling of apical membrane vacuoles than H alone. Cultured gastric glands were examined by differential-interference contrast microscopy at rest and at designated times after stimulation with 200 μM H (*A–D*) alone, 200 μM H plus 20 μM LY (*E–H*), or 200 μM H plus 60 μM IBMX (*I–L*). For all treatments there was an increase in vacuolar area over the 25 min; however, the relative increase was more obvious in the cases where LY or IBMX were included along with H.

membrane area and mitochondrial percent volume remained constant during all treatments, which is the predicted result since these compartments do not significantly change with secretory activity (Table 2). Thus the morphological data, both from direct visualization of parietal cell cultures and high-resolution membrane morphometry, confirm the physiological AP uptake results that the PI3K inhibitor LY significantly stimulates parietal cell secretory response to histamine.

PI3K is not downstream of the EGF receptor in the parietal cell. Short-term exposure of parietal cells to high levels of EGF is known to cause acute inhibition of histamine-stimulated acid secretion (15). Figure 5 shows EGF significantly inhibited histamine stimulation of acid secretion, causing the AP accumulation to go from 2.9 ± 0.4 to 1.5 ± 0.2 ($P < 0.01$). EGF had a similar inhibitory effect on H+LY-stimulated gastric glands where we observed the AP ratio to decrease from 8.3 ± 1.2 to 5.3 ± 1.0 ($P < 0.01$). EGF had no significant effect on maximal stimulation by histamine plus IBMX. These data suggest that LY is not blocking the EGF-mediated pathway. EGF inhibited acid secretion when stimulation was slightly lower and dependent solely on activation of the histamine receptor rather than when the cells were stimulated to a higher degree with histamine plus IBMX.

Table 1. *Morphometric data on vacuolar swelling of stimulated parietal cells*

	No. of Cells	Initial Area, μm²	Final Area, μm²	Percent Increase
H	61	173±14	362±27	136±15
H+LY	63	155±12	402±28	219±32
H+I	49	252±27	615±71	171±19

Data are means ± SE. Measurement of the increase in vacuolar area of parietal cells treated with histamine plus LY (H+LY) shows significant increase over histamine (H) stimulation. Cultured gastric glands were stimulated for 25 min, and DIC images were acquired as described in Fig. 3. The sum of the vacuolar area of each cell was measured using NIH Image. For all treatments there was an increase in vacuolar area over the 25 min; however, the relative increase was more obvious in the cases where LY294002 or IBMX was included along with histamine.

Inhibition of PI3K has no effect on carbachol-mediated acid secretion. Stimulation of acid secretion by gastric glands with carbachol is often found to be relatively low and transient compared with histamine; however, there is a clearly documented spike in the intracellular level of calcium followed by a slightly lower plateau that is likely to be responsible for acid secretory response that is observed (13, 25). Previous studies found high doses of wortmannin (300 nM to 3 μM) inhibited carbachol-stimulated AP accumulation (25). We wanted to examine if the relatively low doses of LY (20 μM) found to enhance histamine stimulation enhanced cholinergic stimulation. For these studies, the effect of LY on the Ca^{2+}/PKC pathway was assayed using carbachol as the agonist for muscarinic receptors on the parietal cell. AP assays on glands treated for 15 min with 100 μM carbachol and with carbachol + LY demonstrated relatively minimal stimulation of

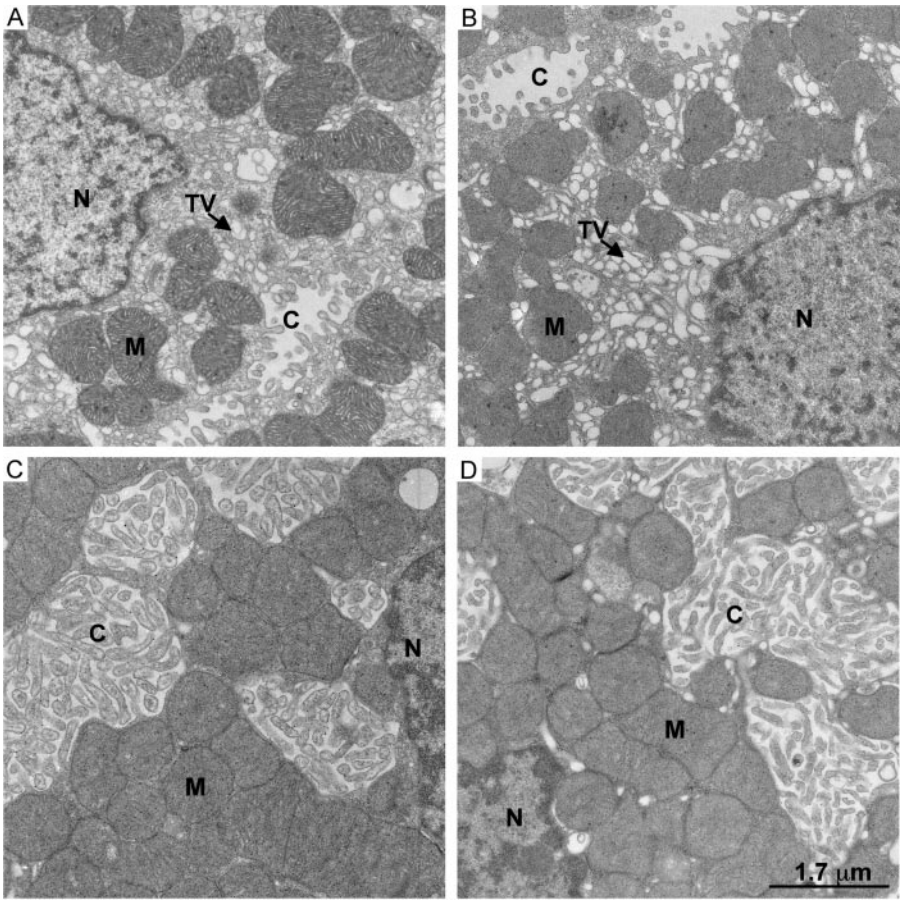

Fig. 4. H+LY exhibits highly stimulated parietal cell morphology. Glands were either held in the resting state with 500 μM Lup (*A*), stimulated with 200 μM H (*B*), 200 μM H plus 60 μM IBMX (*C*), or 200 μM H plus 20 μM LY (*D*) followed by preparation for electron microscopy. These images are typical examples of the apical and canalicular area of parietal cells in the four conditions. Note the decrease in cytoplasmic tubulovesicles (TV) and increase in apical membrane surface area and canalicular (C) area for tissues stimulated with IBMX or LY in addition to H. Nuclei (N) and mitochondria (M) are also indicated.

1.9 ± 0.3-fold and 1.5 ± 0.1-fold over resting, respectively. For comparison, parallel sets of glands treated with 200 μM histamine, 200 μM histamine + 60 μM IBMX, or 200 μM histamine + 20 μM LY for 30 min produced the typical stimulation of 3.5 ± 0.6-fold, 9.0 ± 1.3-fold, and 7.6 ± 1.2-fold over resting levels, respectively ($n \geq 3$ for all experiments). Collectively, these data suggest inhibition of PI3K has little or no effect on acid secretion due to increased intracellular calcium associated with carbachol treatment.

Enhanced stimulation by PI3K inhibitors requires H_2 receptor activation. Given that LY does not appear to alter the actions of EGF or carbachol, the effects of LY on the PKA pathway using agents that typically promote intracellular levels of cyclic AMP were examined. Experiments including dose response data for a variety of cAMP-enhancing agents are summarized in Fig. 6, *A–D*. Gastric glands were treated for 30 min with forskolin to stimulate adenylyl cyclase (Fig. 6*B*), with IBMX to inhibit PDE (Fig. 6*C*), and with dibutyryl cyclic AMP (dbcAMP) to effect intracellular loading with the permeable cAMP analog (Fig. 6*D*). The dose response for each of these agents is compared with that for 30-min histamine (Fig. 6*A*) treatment, both with and without 20 μM LY. Figure 6*A* shows that as histamine concentration was increased to 100 μM, acid secretion also increased. When LY was added to the increasing concentrations of histamine, acid secretion was significantly increased relative to histamine over the full dose range. LY did

Table 2. *Morphometric data on ultrastructure of resting and stimulated gastric glands*

	Surface Area, m^2/cm^2				Percent Volume			
	TV	MV	Apical	BL	TV	MV	Canal	Mito
Lup	2.5±0.2	0.3±0.1	0.4±0.1	0.1±0.02	16±1.2	1.8±0.3	3.1±0.9	28±1.0
H	2.4±0.2	0.3±0.1	0.5±0.1	0.1±0.04	13±1.0	2.0±0.5	4.0±1.4	29±1.0
H+LY	1.1±0.1	1.0±0.2	1.5±0.2	0.1±0.03	5.5±0.7	7.9±1.4	10±2.0	27±1.0
H+I	0.4±0.1	1.5±0.3	2.1±0.3	0.2±0.1	2.3±0.6	11.0±1.5	24±4.4	27±3.0

Data are means ± SE. Quantitative morphometry of parietal cells shows H+LY induces a highly stimulated morphology. Gastric glands were treated for 30 min and then fixed for electron microscopy. Images of well-preserved parietal cells containing at least a portion of the nucleus, apical membrane, and basolateral membrane were taken at a magnification of 9,300x. Surface area and percent of total parietal cell volume were measured using morphometric calculations described in the Methods section. Histamine plus LY394004 (H+LY) significantly increased the apical membrane surface area (Apical, $P < 0.01$) and canalicular volume (Canal, $P < 0.05$) and decreased the tubulovesicular volume (TV, $P < 0.01$) when compared with histamine-treated tissue. Microvillar (MV) surface area and volumes were also determined and increased with H+LY treatment. As expected, little difference was observed between resting and stimulated basolateral membrane (BL) and mitochondria (Mito). $n = 20$ cells.

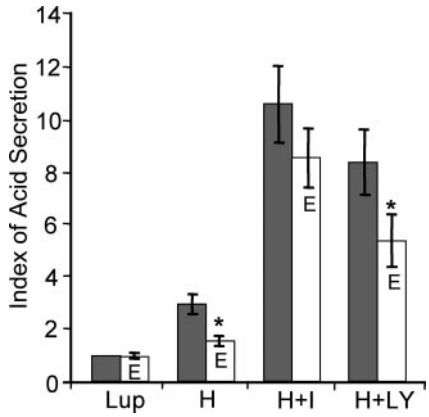

Fig. 5. Epidermal growth factor (EGF) decreases acid secretion stimulated by H+LY. Glands were held in the resting state with 500 μM Lup, AP ratio set at 1.0. Glands were stimulated for 30 min with 200 μM H, 200 μM histamine plus 60 μM IBMX (H+I), or 200 μM histamine plus 20 μM LY294002 (H+LY). EGF, 150 ng/ml (E), was added to half the glands along with the agonists. The addition of EGF significantly inhibited stimulation induced both by H and H+LY, but did not inhibit H+I (*$P < 0.01$). Error bars represent the SE; $n = 10$.

not enhance the stimulatory effects of forskolin (Fig. 6*B*) or dibutyryl cAMP (Fig. 6*D*). For acid secretion stimulated by IBMX, instead of stimulation there was a slight inhibition of glandular AP uptake when LY was added (Fig. 6*C*). These results suggest that for LY to have an additive effect histamine is necessary, implicating the involvement of the histamine receptor in the pathway. To further examine this phenomenon, histamine was included with low doses of forskolin with and without LY. Figure 6*B* shows that low doses of forskolin + histamine have an additive effect resulting in the stimulation of acid secretion up to maximal levels and that the addition of LY does not increase maximal acid secretion when added to forskolin + histamine.

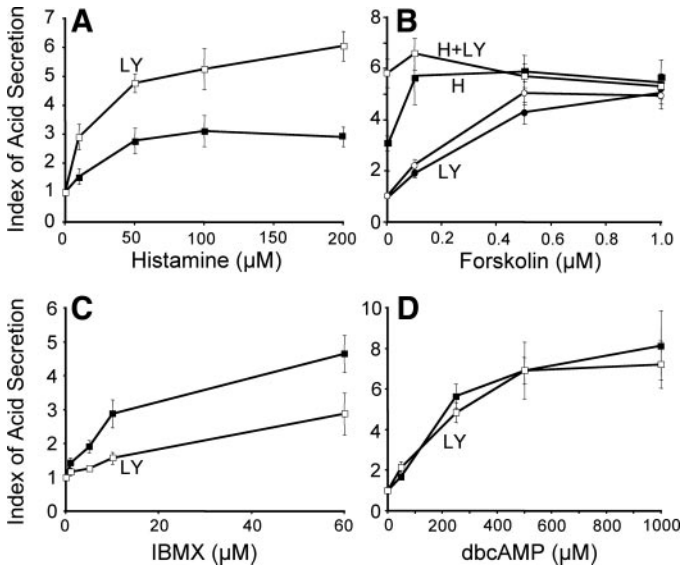

Fig. 6. LY enhances acid secretion stimulated by H but not by forskolin, IBMX, or dbcAMP. Glands were held in the resting state with 500 μM Lup, AP ratio set at 1.0. *A*: glands stimulated for 30 min with H alone and in conjunction with LY. *B*: glands stimulated with forskolin, and in conjunction with LY, H, or H+LY. *C*: Glands stimulated with IBMX and in conjunction with LY. *D*: Glands stimulated with dbcAMP and in conjunction with LY. Error bars represent the SE. $n = 3$ for H, H+LY, IBMX, IBMX+LY, dbcAMP, and dbcAMP+LY; $n = 5$ for forskolin and forskolin+LY.

PI3K inhibition increases histamine-stimulated cAMP levels. Collectively, the above experiments clearly show that inhibition of PI3K in the presence of histamine results in an increased level of stimulation and suggests the H_2 receptor and associated G-coupled protein must be activated for LY to have an effect. Histamine stimulation of the parietal cell increases levels of intracellular cAMP, which peak after 10 min followed by a slightly lower plateau likely due to the activity of PDE (1, 14, 23, 32). Knowing that histamine is required, the morphology of, kinetics of, and maximum level of acid secretion induced by histamine plus LY and by histamine + IBMX are almost identical, we reasoned that the inhibition of PI3K by LY could be causing an increase in cAMP concentration within the parietal cell. To test this hypothesis, the level of cAMP was measured in gastric glands during resting and various stimulated conditions. Although the gastric gland includes cells other than the parietal cell, at least 60% of the total cell volume is parietal cell. The responses to histamine are considered by most investigators to be predominantly those of parietal cells, and it is these secretagogue-induced changes that we have examined here with respect to cAMP and later with respect to Akt phosphorylation. Resting gastric glands have an average of 1.8 ± 0.2 pmol cAMP/mg dry tissue (Table 3). There was a slight but not significant increase in cAMP level, 1.9 ± 0.3 pmol cAMP/mg dry tissue, for histamine-stimulated glands. However, cAMP levels were significantly enhanced when LY was included along with histamine to 3.0 ± 0.3 pmol/mg dry tissue ($P < 0.01$), and cAMP levels were even further elevated by histamine + IBMX to 4.3 ± 0.7 pmol cAMP/mg dry tissue.

Akt is present in gastric glands. A common downstream effector of PI3K is Akt (also referred to as protein kinase B or PKB). Several investigators have shown that PI3K can modulate the activity of PDE and influence the cAMP concentration via Akt, a well-known serine/threonine-specific kinase, by increasing the activity of PDE, possibly via its phosphorylation (16, 21, 28, 29, 39, 41). Accordingly, the activity of endogenous Akt was monitored under various secretory conditions. Cultured gastric glands were held in the resting state or stimulated with histamine, histamine plus IBMX, or histamine + LY as typically performed in earlier experiments. The gland cultures were subsequently solubilized, separated by SDS-PAGE, and blotted to nitrocellulose. Western blots with antibodies against total Akt and H-K-ATPase demonstrate

Table 3. *cAMP levels in resting and stimulated gastric glands*

	cAMP Content, pmol/mg Dry Tissue
Lup	1.8±0.2
H	1.9±0.3
H+LY	3.0±0.3*
H+I	4.3±0.7*

Data are means ± SE. cAMP levels are significantly higher in glands treated with histamine plus LY294002. Freshly isolated glands were held in the resting state with 500 μM lupitidine (Lup) or stimulated with 200 μM histamine (H), histamine plus 60 μM IBMX (H+I), or histamine plus 20 μM LY294002 (H+LY). cAMP levels were assayed as described in Methods. H+LY and H+I stimulated glands have significantly higher levels of cAMP than glands stimulated with histamine alone (* = $P < 0.01$). Error bars represent the SE; $n = 5$.

adequate expression of Akt in the system and relatively even levels of both proteins under all treatments as expected (Fig. 7*A*). On the other hand, Western blots of phosphorylated Akt at serine-473, referred to here as pAkt, demonstrated a great deal of variation depending on treatment. An increase in pAkt occurred when cultured glands were stimulated with histamine and histamine + IBMX. Moreover, there was a dramatic decrease in phosphorylation when PI3K was inhibited with LY during histamine stimulation, indicating that the conditions for LY treatment were having a maximum effect on its target enzyme.

Akt phosphorylation is dependent on histamine and time. To determine whether, and to what extent, Akt was phosphorylated over the normal course of stimulation, Western blot analyses of total Akt and pAkt were performed on freshly isolated gastric glands at 5, 10, 20, and 35 min after treatment with various stimulants. The freely suspended gland preparation was the more typical of those used for many of these experiments and conveniently manipulated for assay of relative pAkt levels. Figure 7*B* shows that within 5 min of treatment with histamine or histamine + IBMX the phosphorylation of Ser^{473} was increased over resting (Lup) levels. Density analyses from four separate experiments indicated that after 10 min of stimulation with either histamine or histamine plus IBMX the phosphorylation of Akt at Ser^{473} was at its maximum, 1.6 ± 0.2 and 1.7 ± 0.1, respectively, and significantly more abundant than resting glands normalized to 1.0 ($P < 0.05$). Interestingly, after 35 min of stimulation a significant decrease in pAkt was observed ($P < 0.05$, Fig. 7*B*). From these data we conclude that 10 min of stimulation was an adequate time of treatment for evaluating the levels of pAkt. The elevated levels of pAkt tended to dissipate or even be reduced below resting with stimulation times of 30 min or greater. Significantly, inhibition of PI3K by LY caused pAkt to greatly decrease within 5 min to 0.3 ± 0.2 and further decreased over the course of stimulation with only trace amounts of pAkt detectable after 35 min. The significant decrease in pAkt after only 5 min of treatment with histamine + LY indicated turnover of phosphate on Ser^{473} was rapid in the gastric glands.

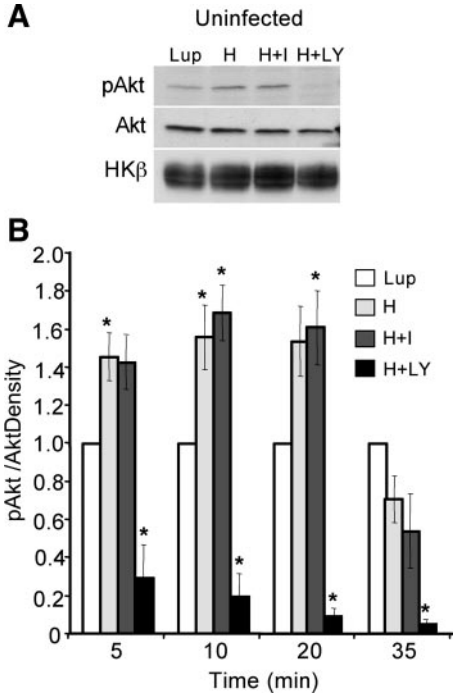

Fig. 7. Akt is present and phosphorylated in a histamine and time dependent manner. Western blot analysis of uninfected cultured gastric glands (*A*, $n = 3$). Time course analysis of pAkt in uninfected glands (*B*, $n = 4$). Cultured gastric glands were held in the resting state with 500 μM Lup or stimulated with 200 μM H, histamine plus 60 μM IBMX (H+I), or histamine + 20 μM LY294002 (H+LY). Western blots were probed for phospho Akt Ser^{473} (pAkt), total Akt (Akt), and H-K-ATPase β-subunit (HKβ), and NIH Image 1.63 was used to determine the area and density of phopho Akt Ser^{473} (pAkt) and total Akt (Akt). Lup set to 1.0. * = $P < 0.05$.

Akt inhibition increases histamine-stimulated acid secretion. To further evaluate Akt as a potential modulator of acid secretion, cultured gastric glands were infected with adenoviral vectors engineered with DNA constructs of wild type Akt (WT-Akt), constitutively active myristoylated Akt (Myr-Akt), or dominant-negative Akt (AAA-Akt) (19), and the response to treatments was evaluated by the immunostaining and AP accumulation assay and by Western blot analyses. Immunostaining of infected glands for HA revealed infection efficiency was greater than 90%, and the morphology was similar to uninfected glands (data not shown). Cultured glands were either held in a resting state or stimulated to secrete acid by histamine. We found that WT- and Myr-Akt effected small but insignificant increases in basal AP accumulation, 5% and 41%, respectively, and AAA-Akt caused a small but insignificant decrease in AP accumulation, 29%. This limited change in the basal level of AP accumulation for infected rabbit glands is in contrast to the large increase (4-fold) in basal AP accumulation reported for Myr-Akt-infected canine parietal cells (34). As a separate control, uninfected cells were stimulated with histamine and showed a 5.7 ± 0.6-fold increase in AP uptake over resting levels, as shown in Fig. 8. Also shown in Fig. 8 are the data for cultured cells that had been infected with the various adenoviral constructs of Akt for 42 h. When the cultured cells were infected with WT- or Myr-Akt, histamine-stimulated acid secretion increased to 4.2 ± 0.7 and 4.8 ± 0.7-fold over resting, respectively. Trends revealed that both WT- and Myr-Akt infected cells stimulated to a lesser degree than uninfected glands. More interestingly, when the cultured cells were infected with the dominant-negative Akt virus AAA-Akt, the AP ratios were greater than uninfected cells and increased significantly over WT- and Myr-Akt infections to 7.5 ± 1.2-fold over resting values ($P < 0.05$, Fig. 8). Western blot analysis of three similar experiments revealed cultured glands infected with any of the three viral constructs resulted in increased expression of total Akt relative to uninfected cultured glands (Fig. 9). Due to the increased expression of total Akt by infected cultured glands, somewhat less sample was loaded relative to uninfected cultured glands. Total Akt and H-K-ATPase expression was not altered with any of the drug treatments, but pAkt varied dramatically. Infection with WT-Akt had high levels of pAkt that were significantly reduced from 6.9 ± 1.24 to 1.8 ± 0.63 when treated with histamine + LY (Fig. 9*B*, $P < 0.05$), whereas Myr-Akt-infected cells did not show a decrease in pAkt with the addition of LY (Fig. 9*C*). The total amount of WT-Akt and Myr-Akt that was phosphorylated at Ser^{473} was markedly greater than uninfected glands, 6.9 ± 1.24, 11.4 ± 1.94, and 1.0, respectively. In cells infected with the AAA-Akt mutant, a low level of pAkt was detected, and this was further diminished in the presence of LY (Fig.

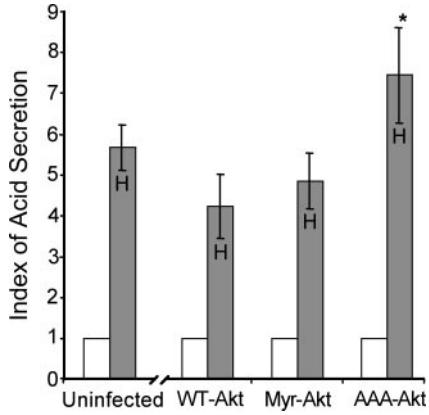

Fig. 8. Inhibition of Akt leads to increased histamine-stimulated acid secretion. AP assays performed on cultured uninfected parietal cells and cells infected with WT-Akt, Myr-Akt, and AAA-Akt adenoviral constructs. Cells were either held in the resting state with 500 μM Lup (white bars), set to 1.0, or stimulated with 200 μM H (gray bars) for 30 min. $n = 5$. * = $P < 0.05$.

9*D*). This observed low level of phosphorylation in the AAA-Akt-infected glands may be due to either a few cells that were not infected, or the AAA-Akt construct may not be completely dominant negative in the gland preparations (e.g., it could be more of a competitive inhibitor). Considering all the above data, we draw the following conclusions: *1*) PI3K inhibition with LY increases acid secretion and prevents Akt phosphorylation; *2*) Overexpression of either WT-Akt or Myr-Akt decreases acid secretion and increases the total amount of pAkt; and *3*) Overexpression of the inactive AAA-Akt mutant results in increased acid secretion and decreased relative phosphorylation. It is clear that PI3K activity is required for Akt phosphorylation and that pAkt results in decreased acid secretion by the gastric parietal cell.

DISCUSSION

The gastric parietal cell is well characterized and is known to perform the important role of HCl secretion into the lumen of the stomach. Multiple cell-signaling pathways carefully regulate this process. Preliminary studies revealed that inhibitors of PI3K had an enhancing effect on acid secretion by isolated gastric glands; we sought to find the basis of this effect.

PI3K inhibition increases histamine-stimulated acid secretion. After our initial observation that LY potentiated AP uptake produced by histamine, we compared this with another commonly used PI3K inhibitor, wortmannin. Interestingly, both inhibitors caused biphasic response in histamine-stimulated acid secretion. Inhibition of acid secretion by wortmannin has been observed previously where high doses inhibited both PKA and myosin light chain kinase (MLCK) resulting in the inhibitory effects (35). It is possible that high doses of LY act in a similar manner, but this has not been addressed here.

To validate that the PI3K inhibitor, LY, was not introducing an artifact into the AP assay, the increased parietal cell activation was verified by two separate morphological approaches. Light microscopy of parietal cells in culture and high-resolution electron microscopy on gastric glands confirmed that LY potentiated the secretory response to histamine.

Enhanced stimulation by PI3K inhibition requires H_2 receptor activation. It was only when the H_2 receptor was occupied by an agonist that the enhancing secretory effect was seen. For example, the PI3K inhibitor had no potentiating effect when cAMP was elevated by forskolin, dbcAMP, or IBMX without histamine. (In fact, in the latter case LY tended to reduce acid output.) Inhibition of PI3K has no effect on resting glands or glands maximally stimulated with histamine plus IBMX. It is now commonly accepted that histamine is the main stimulant of the gastric parietal cell (8, 10). Stimulation begins with the agonist, histamine, binding to the G coupled-protein H_2 receptor, dissociating the Gαβγ complex, and causing the Gα subunit to activate adenylyl cyclase, thus increasing the intracellular cAMP level, the activation of PKA, and the phosphorylation of numerous proteins responsible for the trafficking and recruitment of H-K-ATPase-rich tubulovesicles to the apical membrane (14, 17). Interestingly, when parietal cells from either rabbit or newborn pig are stimulated with histamine, cAMP levels peak after ~10 min followed by a lower level steady state that lasts ~30 min (1, 14, 23). The lower steady state level has been proposed to be due to the activity of PDE because the addition of IBMX, a PDE inhibitor, results in higher levels of cAMP and prevents the lower steady state (23, 32). We propose a link between histamine activation of the PI3K/Akt pathway and the activity of PDE leading to decreased cAMP levels during histamine stimulation. The phosphorylation and thus activation of Akt via PI3K correlates with cAMP levels. The data gathered in this study clearly demonstrate PI3K plays an important regulatory role of cAMP levels during histamine stimulation.

PI3K activity does not alter acute effects of EGF. Signaling in the parietal cell is complicated by the acute inhibition by agents such as somatostatin (22) and EGF (15). Somatostatin works directly on parietal cells by binding the somatostatin 2

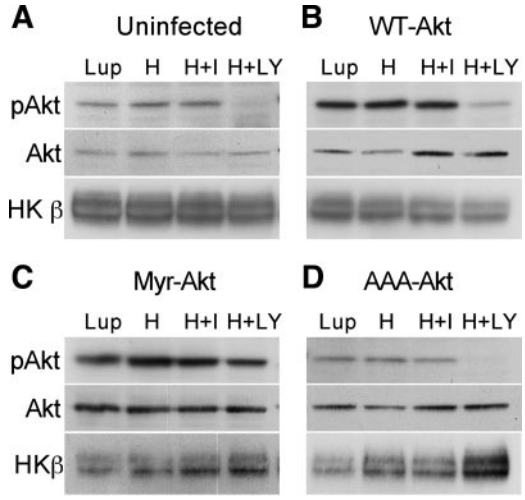

Fig. 9. H+LY drastically decreases phosphorylation in all treatments except the constitutively active Myr-Akt. WT-Akt and Myr-Akt are highly phosphorylated, whereas AAA-Akt has limited phosphorylation. Infected cells express higher levels of total Akt than uninfected cells. All are cultured gastric glands shown as (*A*) Uninfected, (*B*) WT-Akt infected, (*C*) Myr-Akt infected, and (*D*) AAA-Akt infected. The cultured glands were held in the resting state with 500 μM Lup or stimulated with 200 μM H, histamine plus 60 μM IBMX (H+I), or histamine + 20 μM LY294002 (H+LY) for 10 min. Western blots were probed for phosphorylated Akt at serine-473 (pAkt), total Akt (Akt), and H-K-ATPase β-subunit(HKβ). $n = 3$.

receptor inhibiting adenylyl cyclase via the GPCR α_i-subunit (3, 27, 30). EGF reduces acid output via EGF receptors and downstream protein tyrosine kinase, not PI3K (15, 25). PI3K is also often found associated with, and operating downstream of, the EGF receptor. Data here do not directly address that continuity, but they are generally consistent with the hypothesis that the inhibitory effects of EGF are manifest at relatively low levels of cAMP and become diminished or totally abrogated as cellular cAMP is enhanced (15). Consistent with this idea, we observed no effect of EGF at maximal cAMP levels generated by H + I, a relatively smaller percent inhibition at somewhat lower levels of cAMP generated by H + LY, and almost complete inhibition of acid secretion at the low level of cAMP associated with stimulation by histamine alone. In addition to such acute inhibition, EGF has also been reported to have a chronic enhancing effect on acid secretion (15). EGF appears to have complex influences on the development of parietal cells, regulating expression of the proton pump via an Akt-mediated pathway during later stages of EGF exposure (33, 34). It appears as though the acute early inhibition of histamine-stimulated acid secretion by EGF is not dependent on PI3K/Akt stimulation of H-K-ATPase gene expression (25), but rather competition between the housekeeping chores performed by growth factor stimulation and the acid secretion stimulated by histamine.

PI3K inhibition of histamine-stimulated acid secretion requires Akt. The data presented here indicate: *1*) Histamine stimulation increases Akt phosphorylation; *2*) PI3K inhibition with LY increases histamine-stimulated acid secretion, intracellular cAMP levels, and prevents Akt phosphorylation; and *3*) Overexpression of WT-Akt or Myr-Akt decreases acid secretion and increases the total amount of pAkt, whereas overexpression of the inactive AAA-Akt mutant results in increased histamine-stimulated acid secretion and decreased relative phosphorylation. Taken together, the following conclusions can be drawn: PI3K activation by histamine leads to the phosphorylation of Akt, which in turn lowers the cAMP levels in the cell, reducing acid secretion. PDE is responsible for the breakdown of cAMP into AMP and is known to play a role in regulating levels of cAMP in the gastric parietal cell (17). We propose that PI3K activity leads to Akt phosphorylation during histamine stimulation and that Akt activation alters the activity of PDE, thereby lowering the level of cAMP. In other tissues PI3K has been observed to alter cAMP levels through Akt and PDE. Activation of PI3Kγ by the β-adrenergic receptor 2 GPCR leads to decreased levels of cAMP in cardiomyocytes (16). Studies on heart contractility suggest that PI3Kγ increases PDE activity via $p87^{PIKAP}$ and lowers the level of cAMP (28, 39). The interplay between PI3K and PDE has also been observed in both adipocytes and pancreatic β-cells, where respective agonist binding to receptor tyrosine kinase activates PI3K leading to an increase in PDE phosphorylation and activation (21, 41). Kitamura et al. (21) further showed that Akt is responsible for the phosphorylation of PDE in a PI3K-dependent manner (21). From data in this study and what can be inferred from the role of PI3K in insulin signaling and cardiac contraction, it is likely that activation of the H_2 receptor leads to stimulation of PI3K via the GPCR and that PI3K activation results in phosphorylation of Akt. Once activated, Akt can stimulate the activity of PDE and thereby lower the level of cAMP in the gastric parietal cell.

PI3K, a negative regulator of histamine-stimulated acid secretion. The role of PI3K in the gastric parietal cell is still under investigation, but evidence presented here demonstrates that PI3K is involved in the regulation of intracellular cAMP levels and in turn the degree of acid secretion. We offer Fig. 10 as a schematic model to account for interactions between the PI3K and the histamine/protein kinase A pathway regulating acid secretion. A summary of support for the model is as follows: *1*) Inhibition of PI3K (LY) potentiates histamine-mediated acid secretion, as validated here by several methods. *2*) Potentiation of secretion by LY is also associated with elevated levels of cAMP, and *3*) it appears to require the H_2 G-protein coupled receptor since other means to elevate cAMP do not give rise to the potentiation. *4*) Akt is a downstream target of PI3K, and *5*) others have shown that PDE activation is a targeted process of Akt (16, 21, 28, 39, 41). From data on the incorporation of Akt constructs into parietal cells, we demonstrate that *6*) histamine stimulates phosphorylation of Akt and that *7*) this process is virtually completely abolished by LY. *8*) A form of Akt that acts as a negative influence on Akt function significantly elevates histamine-stimulated AP uptake. Furthermore, we propose that when histamine binds to the H_2 receptor the Gα- and G$\beta\gamma$-subunits dissociate and that the G$\beta\gamma$-subunit activates PI3K (Fig. 10). PI3K phosphorylates PIP_2 producing PIP_3, which in turn recruits Akt to the membrane where it is activated (Fig. 10). Once phosphorylated, Akt can return to the cytosol and activate PDE and decrease cAMP levels. There is still little understanding of the cross talk between all the pathways and how the parietal cell coordinates them to perform vital housekeeping chores as well as the secretory response. Some of these important regulatory mechanisms are slowly percolating to an understanding as the tools for evaluating the pathways are expanding. Nonetheless, the

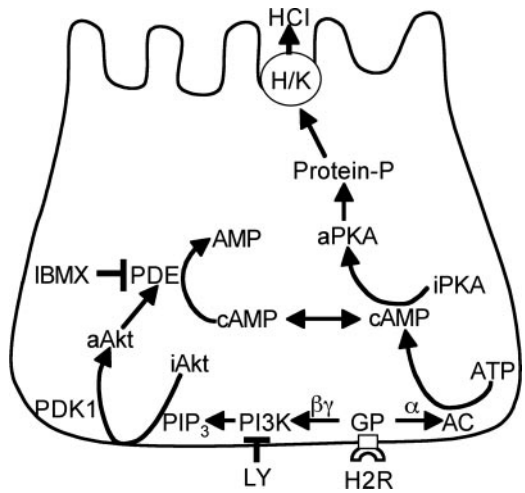

Fig. 10. Proposed scheme for stimulation of phosphodiesterase (PDE) by histamine receptor activation of PI3K. H binds the H_2 receptor (H2R) activating the trimeric G$\alpha\beta\gamma$ coupled protein (GCP). Dissociated G$\beta\gamma$ subunits activate PI3K, increasing the concentration of phosphoinositide 3,4,5-phosphate (PIP_3) and recruiting inactive Akt (iAkt) to the membrane. Akt is phosphorylated by PDK1 and TORC2 (latter not shown). Phosphorylated Akt (aAkt) returns to the cytosol and activates PDE. PDE decreases the cAMP level in the cell, decreasing parietal cell stimulation. In addition to the proposed PI3K/Akt pathway, the standard histaminergic pathway is shown, including adenylyl cyclase (AC) and cAMP activation of PKA. Thus inhibition of PI3K by LY relaxes the negative modulation of cAMP levels.

present studies indicate a role for PI3K as a negative modulator of histamine-stimulated acid secretion in the parietal cell.

ACKNOWLEDGMENTS

We thank Dr. K. Walsh for the viral constructs: wild-type mouse Akt (WT-Akt), myristoylated Akt (Myr-Akt), and Akt mutated by substitutions at Lys179Ala, Thr308Ala, and Ser473Ala (AAA-Akt) (19). We thank Dr. T. Machen for the Bosc 23 cells.

GRANTS

This work was supported by a grant from the U.S. Public Health Service, DK10141.

REFERENCES

1. **Adrian TE, Goldenring JR, Oddsdottir M, Zdon MJ, Zucker KA, Lewis JJ, Modlin IM.** A micromethod for the assay of cellular secretory physiology: application to rabbit parietal cells. *Anal Biochem* 182: 346–352, 1989.
2. **Agnew BJ, Duman JG, Watson CL, Coling DE, Forte JG.** Cytological transformations associated with parietal cell stimulation: critical steps in the activation cascade. *J Cell Sci* 112: 2639–2646, 1999.
3. **Allen JP, Canty AJ, Schulz S, Humphrey PP, Emson PC, Young HM.** Identification of cells expressing somatostatin receptor 2 in the gastrointestinal tract of Sstr2 knockout/lacZ knockin mice. *J Comp Neurol* 454: 329–340, 2002.
4. **Athmann C, Zeng N, Scott DR, Sachs G.** Regulation of parietal cell calcium signaling in gastric glands. *Am J Physiol Gastrointest Liver Physiol* 279: G1048–G1058, 2000.
5. **Berglindh T, Helander HF, Obrink KJ.** Effects of secretagogues on oxygen consumption, aminopyrine accumulation and morphology in isolated gastric glands. *Acta Physiol Scand* 97: 401–414, 1976.
6. **Berglindh T, Obrink KJ.** A method for preparing isolated glands from the rabbit gastric mucosa. *Acta Physiol Scand* 96: 150–159, 1976.
7. **Black JA, Forte TM, Forte JG.** Inhibition of HCl secretion and the effects on ultrastructure and electrical resistance in isolated piglet gastric mucosa. *Gastroenterology* 81: 509–519, 1981.
8. **Black JW, Duncan WA, Durant CJ, Ganellin CR, Parsons EM.** Definition and antagonism of histamine H_2-receptors. *Nature* 236: 385–390, 1972.
9. **Blakemore RC, Brown TH, Durant GJ, Ganellin CR, Parsons ME, Rasmussen AC, Rawlings DA.** SK&F 93479, a potent and long acting histamine H_2-receptor antagonist. *Britsh Journal of Pharmacology* 74: 200, 1981.
10. **Brimblecombe RW, Duncan WA, Durant GJ, Emmett JC, Ganellin CR, Leslie GB, Parsons ME.** Characterization and development of cimetidine as a histamine H_2-receptor antagonist. *Gastroenterology* 74: 339–347, 1978.
11. **Chew CS.** Forskolin stimulation of acid and pepsinogen secretion in isolated gastric glands. *Am J Physiol Cell Physiol* 245: C371–C380, 1983.
12. **Chew CS.** Parietal cell protein kinases. Selective activation of type I cAMP-dependent protein kinase by histamine. *J Biol Chem* 260: 7540–7550, 1985.
13. **Chew CS, Brown MR.** Release of intracellular Ca2+ and elevation of inositol trisphosphate by secretagogues in parietal and chief cells isolated from rabbit gastric mucosa. *Biochim Biophys Acta* 888: 116–125, 1986.
14. **Chew CS, Hersey SJ, Sachs G, Berglindh T.** Histamine responsiveness of isolated gastric glands. *Am J Physiol Gastrointest Liver Physiol* 238: G312–G320, 1980.
15. **Chew CS, Nakamura K, Petropoulos AC.** Multiple actions of epidermal growth factor and TGF-alpha on rabbit gastric parietal cell function. *Am J Physiol Gastrointest Liver Physiol* 267: G818–G826, 1994.
16. **Crackower MA, Oudit GY, Kozieradzki I, Sarao R, Sun H, Sasaki T, Hirsch E, Suzuki A, Shioi T, Irie-Sasaki J, Sah R, Cheng HY, Rybin VO, Lembo G, Fratta L, Oliveira-dos-Santos AJ, Benovic JL, Kahn CR, Izumo S, Steinberg SF, Wymann MP, Backx PH, Penninger JM.** Regulation of myocardial contractility and cell size by distinct PI3K-PTEN signaling pathways. *Cell* 110: 737–749, 2002.
17. **Forte JG.** Gastric function. In: *Comprehensive Human Physiology*, edited by Greger R and Windhorst U. Berlin Heidelberg: Springer-Verlag, 1996, p. 1239–1257.
18. **Forte TM, Machen TE, Forte JG.** Ultrastructural changes in oxyntic cells associated with secretory function: a membrane-recycling hypothesis. *Gastroenterology* 73: 941–955, 1977.
19. **Fujio Y, Guo K, Mano T, Mitsuuchi Y, Testa JR, Walsh K.** Cell cycle withdrawal promotes myogenic induction of Akt, a positive modulator of myocyte survival. *Mol Cell Biol* 19: 5073–5082, 1999.
20. **Ito S, Schofield GC.** Studies on the depletion and accumulation of microvilli and changes in the tubulovesicular compartment of mouse parietal cells in relation to gastric acid secretion. *J Cell Biol* 63: 364–382, 1974.
21. **Kitamura T, Kitamura Y, Kuroda S, Hino Y, Ando M, Kotani K, Konishi H, Matsuzaki H, Kikkawa U, Ogawa W, Kasuga M.** Insulin-induced phosphorylation and activation of cyclic nucleotide phosphodiesterase 3B by the serine-threonine kinase Akt. *Mol Cell Biol* 19: 6286–6296, 1999.
22. **Komasaka M, Horie S, Watanabe K, Murayama T.** Antisecretory effect of somatostatin on gastric acid via inhibition of histamine release in isolated mouse stomach. *Eur J Pharmacol* 452: 235–243, 2002.
23. **Machen TE, Rutten MJ, Ekblad EB.** Histamine, cAMP, and activation of piglet gastric mucosa. *Am J Physiol Gastrointest Liver Physiol* 242: G79–G84, 1982.
24. **Mangeat P, Gusdinar T, Sahuquet A, Hanzel DK, Forte JG, Magous R.** Acid secretion and membrane reorganization in single gastric parietal cell in primary culture. *Biol Cell* 69: 223–231, 1990.
25. **Nakamura K, Zhou CJ, Parente J, Chew CS.** Parietal cell MAP kinases: multiple activation pathways. *Am J Physiol Gastrointest Liver Physiol* 271: G640–G649, 1996.
26. **Negulescu PA, Reenstra WW, Machen TE.** Intracellular Ca requirements for stimulus-secretion coupling in parietal cell. *Am J Physiol Cell Physiol* 256: C241–C251, 1989.
27. **Park J, Chiba T, Yamada T.** Mechanisms for direct inhibition of canine gastric parietal cells by somatostatin. *J Biol Chem* 262: 14190–14196, 1987.
28. **Patrucco E, Notte A, Barberis L, Selvetella G, Maffei A, Brancaccio M, Marengo S, Russo G, Azzolino O, Rybalkin SD, Silengo L, Altruda F, Wetzker R, Wymann MP, Lembo G, Hirsch E.** PI3Kgamma modulates the cardiac response to chronic pressure overload by distinct kinase-dependent and -independent effects. *Cell* 118: 375–387, 2004.
29. **Rahn T, Ridderstrale M, Tornqvist H, Manganiello V, Fredrikson G, Belfrage P, Degerman E.** Essential role of phosphatidylinositol 3-kinase in insulin-induced activation and phosphorylation of the cGMP-inhibited cAMP phosphodiesterase in rat adipocytes. Studies using the selective inhibitor wortmannin. *FEBS Lett* 350: 314–318, 1994.
30. **Schepp W, Schmidtler J, Dehne K, Schusdziarra V, Classen M.** Pertussis toxin-sensitive and pertussis toxin-insensitive inhibition of parietal cell response to GLP-1 and histamine. *Am J Physiol Gastrointest Liver Physiol* 262: G660–G668, 1992.
31. **Soll AH.** Extracellular calcium and cholinergic stimulation of isolated canine parietal cells. *J Clin Invest* 68: 270–278, 1981.
32. **Soll AH, Wollin A.** Histamine and cyclic AMP in isolated canine parietal cells. *Am J Physiol Endocrinol Metab Gastrointest Physiol* 237: E444–E450, 1979.
33. **Stepan V, Pausawasdi N, Ramamoorthy S, Todisco A.** The Akt and MAPK signal-transduction pathways regulate growth factor actions in isolated gastric parietal cells. *Gastroenterology* 127: 1150–1161, 2004.
34. **Todisco A, Pausawasdi N, Ramamoorthy S, Del Valle J, Van Dyke RW, Askari FK.** Functional role of protein kinase B/Akt in gastric acid secretion. *J Biol Chem* 276: 46436–46444, 2001.
35. **Urushidani T, Muto Y, Nagao T, Yao X, Forte JG.** ME-3407, a new antiulcer agent, inhibits acid secretion by interfering with redistribution of H(+)-K(+)-ATPase. *Am J Physiol Gastrointest Liver Physiol* 272: G1122–G1134, 1997.
36. **Vanhaesebroeck B, Leevers SJ, Ahmadi K, Timms J, Katso R, Driscoll PC, Woscholski R, Parker PJ, Waterfield MD.** Synthesis and function of 3-phosphorylated inositol lipids. *Annu Rev Biochem* 70: 535–602, 2001.
37. **Vanhaesebroeck B, Leevers SJ, Panayotou G, Waterfield MD.** Phosphoinositide 3-kinases: a conserved family of signal transducers. *Trends Biochem Sci* 22: 267–272, 1997.
38. **Vlahos CJ, Matter WF, Hui KY, Brown RF.** A specific inhibitor of phosphatidylinositol 3-kinase, 2-(4-morpholinyl)-8-phenyl-4H-1-benzopyran-4-one (LY294002). *J Biol Chem* 269: 5241–5248, 1994.
39. **Voigt P, Dorner MB, Schaefer M.** Characterization of p87PIKAP, a novel regulatory subunit of phosphoinositide 3-kinase gamma that is

highly expressed in heart and interacts with PDE3B. *J Biol Chem* 281: 9977–9986, 2006.

40. **Wymann MP, Bulgarelli-Leva G, Zvelebil MJ, Pirola L, Vanhaesebroeck B, Waterfield MD, Panayotou G.** Wortmannin inactivates phosphoinositide 3-kinase by covalent modification of Lys-802, a residue involved in the phosphate transfer reaction. *Mol Cell Biol* 16: 1722–1733, 1996.
41. **Zhao AZ, Zhao H, Teague J, Fujimoto W, Beavo JA.** Attenuation of insulin secretion by insulin-like growth factor 1 is mediated through activation of phosphodiesterase 3B. *Proc Natl Acad Sci U S A* 94: 3223–3228, 1997.
42. **Zhou R, Zhu L, Kodani A, Hauser P, Yao X, Forte JG.** Phosphorylation of ezrin on threonine 567 produces a change in secretory phenotype and repolarizes the gastric parietal cell. *J Cell Sci* 118: 4381–4391, 2005.